Realization of a Faster, Cheaper, Better Star Tracker for the New Millennium

Allan Read Eisenman
Jet Propulsion Laboratory
4800 Oak Grove Dr.
Pasadena, CA 91109
818354-4999
allan.eisenman@jpl.nasa.gov

Carl Christian Liebe
Technical University of Denmark
2s001 Lyngby, Denmark
45-45-25-34-39
ccl@iau.dtu.dk

John Leif Jørgensen
Technical University of Denmark
28001 Lyngby, Denmark
45-45-25-34-48
jlj@iau.dtu.dk

Gunnar Bent Jensen
Technical University of Denmark
2800 Lyngby, Denmark
4s-45-2s-34.46

Abstract- The Advanced Stellar Compass (ASC) is a second generation star tracker consisting of a CCD camera and its associated microcomputer. It is a true, multi-star tracker which was dc.signed for the Ørsted mission, a precision mapper of the Earth's magnetic field. The ASC operates by matching the star images acquired by the camera to internal star catalogs. An initial attitude acquisition (solving the lost in space. problem) is performed, and then the attitude of the camera is calculated in celestial coordinates by averaging the position of a large number of stat observations for each image. The ASC features high accuracy, a smooth response. to changing star fields, high boresight stability, low power and mass, robust autonomy, quaternion output and low cost. It is readily adapted to a wide range of missions, four of which arc cited. Key parameters of the ASC for the Ørsted and Astrid II satellites are: mass as low as 900 g; power consumption as low as 5.5 W; a single. axis, relative, attitude angle error of less than 1,4 arcsec, I< MS, and a twist, or roll angle, relative. accuracy of less than 13 arcsec, I< MS, as measured at the Mauna Kea, Hawaii observatories of the University of Hawaii in June 1996.

TABLE OF CONTENTS

1. INTRODUCTION, THE ØRSTED MISSION

The Danish geomagnetic research satellite. Ørsted [1] is an autonomous micro satellite.

The objective of the satellite is to perform a precision global survey of the magnetic field of the Earth. This will enable scientists to evaluate the internal field of the 1 Earth and to compare it to earlier models of the core field. The last global survey of the magnetic field was done in the late 1970's by the NASA/GSFC Magsat satellite.. The Ørsted satellite is shown in Fig. 1.

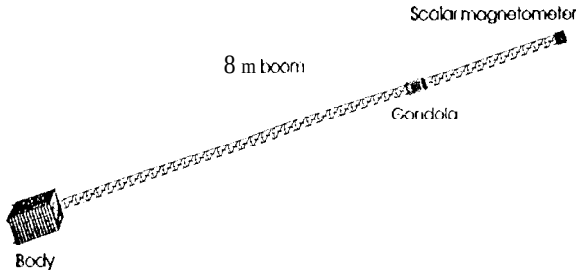

Figure 1. The Ørsted satellite.

The design of the Ørsted satellite was initiated in 1993 and it belongs to a new generation of highly autonomous missions. It is a successful example of realizing a faster, cheaper, better design. The satellite. is sponsored by the 1 Danish Government, NASA, CNES and DARA. The project has take.1] approximately 3 years from concept to delivery of the. flight system, and the total costs (including operations) arc approximately $35M (F Y97), not including some academic support labor costs.

The Ørsted payload includes: a vector magnetometer (3-axis, flux gate sensor of the compact spherical coil type [?]); a scalar magnetometer (Overhauser, enhanced, proton precession magnetometer [3]); an energetic particle detector (3 energy band [4]) and an advanced stellar compass, or ASC (a fully autonomous star tracker [5]).

Table 1 lists major parameters of the micro satellite.

In order for the vector magnetometer to be useful, it requires very accurate pointing information. This is provided by the ASC. Therefore, the. vector magnetometer is mounted together with the. ASC on a SiSiC optical bench, the Gondola, as shown in Fig. ?.

'1'able 1. Major parameters of the Ørsted satellite

Parameter	Value
Mass	61.4 kg
Width	45 cm
1)epth	34 cm
Height	68 cm
Boom	8 m
Power	Solar panels/t)atkrics 54/22 W, average
Stabilization	Gravitation/magnetic torquers
Orbit	Polar 450 x 850 km

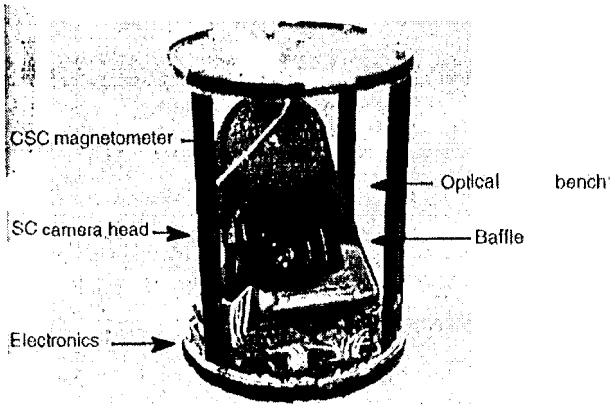

Figure 2. The Ørsted gondola.

2. The Advanced Stellar Compass Concept

The only practical way to meet the 20 arcsec, 1 σ, attitude knowledge requirement of the vector magnetometer, is to use a star tracker. This is true because star trackers use the highest-accuracy available, attitude. reference system, the celestial coordinates of the firmament. Since the. intrinsic, catalog accuracy of a star is about 0.3 arcsec, RMS, the. limiting accuracy of a stellar reference is more than sufficient. The ASC greatly exceeds the attitude knowledge needs of the vector magnetometer with a relative accuracy of 1.4 arcsec, RMS, single axis, as confirmed in real sky tests, with the flight camera head of 12.7 g mass and 0.4 W power consumption.

An additional requirement for the Ørsted star tracker is that it be nonmagnetic, in order not to interfere with magnetic field measurements. A 1993 survey disclosed that no commercial

star trackers were able to meet the requirements of magnetic cleanliness, low mass and low power consumption. Therefore, a new design had to be undertaken and the. 'J'ethnical University of Denmark was chosen to design and build the instrument. Subsequently, as part of its support of the Ørsted mission, NASA Code YSG funded J})l. to conduct an independent evaluation of the ASC.

The ASC is separated into two units, the Camera Head Unit (CHU) and the Data Processing Unit (DPU). The function of the CI 1 U is to deliver star field image frames to the DPU. The function of the DPU is to compare. the images from the CHU with one of the two, onboard, star catalogs in order to identify the stars in its field of view (FOV) and then, to determine the pointing direction and the twist angle of the CHU about its boresight. The CHU is shown in Fig. 3.

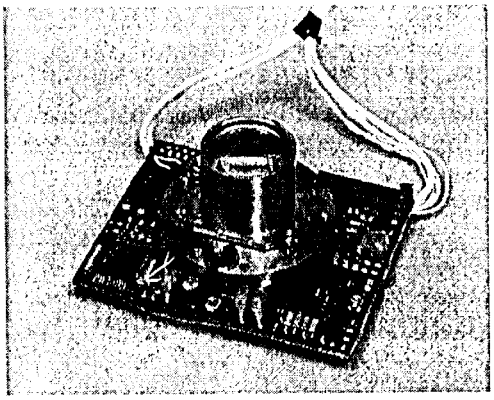

Figure 3. The Ørsted CHU.

It should be emphasized that there is a significant difference between a conventional star tracker and the ASC. A conventional star tracker typically consists of a star camera with integral electronics. It detects a small number of bright images on the. CCD sensor and outputs the coordinates of these images relative to the CCD. The ASC, on the other hand, transfers the entire image from the CHU to the 1)11 U, where the bright images detected by the. CCD are directly compared to a star catalog and the absolute pointing direction of the CHU is output in the form of a quaternion.

In order to provide the robust autonomy and high accuracy demanded by the mission, the ASC detects and tracks a large number of stars per image frame. The typical number is 65 with a range from 25 to 200.

The output quaternion is based on averaging the positions of all of the tracked stars, thus reducing the random errors of each star position by the square root of the number being tracked.

The combination of features qualifies the ASC as the first example of a new, second generation type of solid state, CCD based star trackers. The old generation used "windowed" tracking of a small number of stars (typically 3 to 5) and no internal star catalogs nor autonomy.

The ASC separation of the detection and the processing functions of a star tracker confers a number of advantages. The very low mass of the CHU permits a precision, kinematic, ball mount with a boresight stability in the arcsecond range. This is about 20 times better than first generation mounting systems. The low power and compact size of the CHU result in inherently stable thermal mechanical properties which further enhance pointing stability. The low power consumption also greatly simplifies temperature control. The separate processor may be readily customized for particular missions or eliminated altogether by implementing its functions in a powerful, integrated, central attitude controlling computer.

The ASC is readily adapted to a variety of missions. Key parameters of it and its mission variants are given in '1'able 2.

3. The CHU

The CHU is based on a commercial, interline, microlens fitted CCD, the SONY CI)X039AI and its support chip set. The CCD has a resolution of 752 x 582 pixels, each with a dimension of 8.6 µm x 8.3 µm. The imaging lens is a customized, 7 element double Gauss type with an integral field flattener. The focal ratio is f/0.7 with a 16.4 mm focal length, and a 380 nm to 850 nm spectral bandpass filter coating. It has 4 times the light gathering power of the conventional f/1.7 star tracker lens. It was designed to minimize chromatic

distortion and at the same time yield a controlled and limited point spread function of so µm diameter over the entire FOV. The FOV is 22° by 16°, or approximately 1/12.0 of the entire firmament. The CHU has a software settable image integration time, with a default value of 1 second, resulting in a readout noise level of 10 electrons. The high speed lens, the CCD sensitivity and the 1 sec integration time result in signal of 45 electrons per pixel for a star with an instrument magnitude of 6.0.

Table 2. Key parameters of the ASC and its variants

PARAMETERS	Ø(M)	AII(P)	I(T)	HP(M)
Star sensitivity threshold, M_1	6.0	4.(J	6.(J	9.5
Acquisition data base, number of stars	2,200	TBD	2,200	42,654
Tracking data base, number of stats	10,301	TBD	10,301	231,43S
Noise equivalent angle, 1 axis, RMS, arsec (A)	1.0	1,5	1.5	<0.1 (s)
Relative accuracy, axis, RMS error, arcsec (A)	1.4	2.1	2.0	0.54
Mass, camera head, Kg (excluding baffle)	0.13	0.20	0.45	<2.0
Mass, processing electronics, Kg	1.4	0.80	0.90	1.0
Power consumption, camera head, W	0.5	0.4	0.4	0.4
Power consumption, proc. elec's, W	5.0	7.0	6.0	11.0
Field of view, degrees	16X22	16X22	16x22	33 X4..?
Update rate, Hz	1	2	2	1
Permissible radiation dosage, KRad	10	10	100	20

Ø= Ørsted; AII= ASTRID 11; HP= High Precision; I= Interplanetary; A= without image motion smear; M: measured at Mauna Kea, 6/96; P= projected; S= staring mode; T= measured at J1'17J'MO, 8/96

4. THE DPU

The DPU consists of a 80486 based processor board, a digitizer, anti a digital interface. The analog image from the CHU is digitized and stored in its frame grabber. All communications arc. routed via an RS422 telemetry interface. The processor is an AMD 80486 with a 9519 support chip. Its clock rate is 20M hz for Ørsted and 100 Mhz for ASTRID II. The processor is equipped With 4 Mbytes of 1)RAM and 4 Mbytes of flash RAM and a radiation resistant, fuse.-linkcd bootprom. All electronics are protected against single event setup by current measuring circuits. The flash RAM utilizes hamming coding to avoid bit flips and at regular intervals the CPU performs bit washes to avoid double faults.

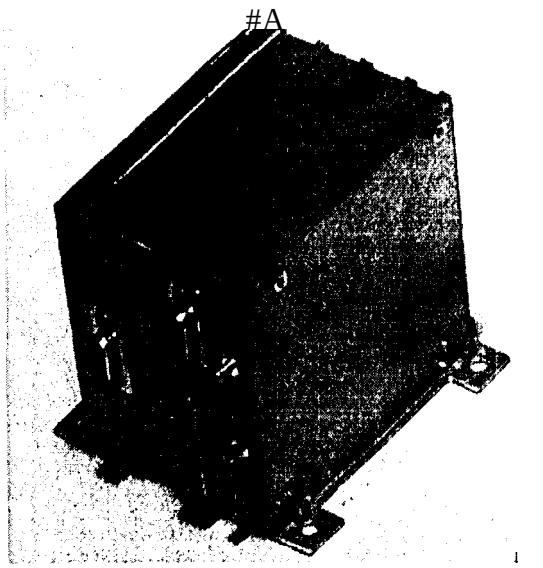

Figure 4. The ASTRID II DPU

5. ASC OPERATION

The ASC operates in two modes: initial attitude acquisition and tracking mode.

The initial attitude acquisition mode is automatically entere d when n o prior knowledge of the CHU pointing direction exists. Typically, this occurs after power on, or whenever the attitude lock is lost.

The tracking mode (normal operation) is automatically entered whenever an approximate attitude is known (e. g., the previous attitude).

The operational flow of the ASC is:

- Image acquisition
- initial attitude acquisition
- Tracking
- Attitude estimate verification

If the attitude calculation is satisfactory, the sequence is repeated, without the initial attitude acquisition, based on the previous attitude estimate. If the sequence is disturbed in any manner, including receipt of an external reset command, the ASC automatically reverts to the acquisition mode.

During initial attitude acquisition, the star centroids arc analyzed for triplet angle sets based on the nearest and second nearest neighbors of the star being identified. The resulting set of triplets is then matched to a preflight compiled version of the star catalog, which is the star database. The entries in the star database include all possible star triplets. Based cm this match, an attitude is obtained which is used in the subsequent processing [6,7].

As soon as the initial attitude acquisition algorithm has established an approximate attitude value, all useable stars in the FOV are correlated with stars from the tracking catalog. '1'hen, a spherical, nonlinear, least squares fit (1 .SF)[8] is performed with very high precision.

1 During normal operation, the ASC update rate of 1 Hz ensures that images from the previous frame have only minor position shifts during spacecraft, 3-axis, stabilized operation. 1 lence, to save power, only the. I .SF algorithm needs to be invoked to obtain high precision attitude estimates for each image, while in the tracking mode.

Should the attitude. rate of change be.come excessive, or should some other event make the LSF algorithm divert from the correct solution, the LSF residual will exceed a preset value, and the initial attitude acquisition algorithm is invoked again, autonomously.

Finally, the attitude is corrected for light time aberration (by an intro nal orbit model, updated by GPS input) and the quaternion is transferred to the telemetry queue.

6. Components of Accuracy

The effect of noise on attitude errors is a unique, characteristic of each particular star tracker design. 'l'his is especially true for a complex instrument such as the ASC. The error and noise impacts on the ASC have. been established through various measurements and tests. in order clarify the terminology and to organize the specific error and noise contributions into a usable form, the error budget terms can be placed in the broad categories of NEA, relative accuracy and boresight bias, which then combine to form the absolute accuracy of a star tracker, which will degrade over its lifetime.

NEA

When the ASC is presented with the same stimuli of an unchanging star field, repeatedly during staring operations, the calculated attitude will differ from image to image, even though the input is constant. This is clue to various noise sources such as photon statistics, amplifier noise, dark current noise, etc. The resulting attitude, jitter will appear on the same time scale as the 'integration time. of the ASC. This error is defined as the noise equivalent angle. (NEA).

Pointing accuracy of a fixed scene is largely limited by the NEA. The NJ EA is characterized by high frequency noise terms.

Relative Accuracy

Other error sources can also affect the short term accuracy, depending on the usc of the ASC. When the ASC is subjected to an image sequence from a spacecraft maneuver, or a

changing star field caused by spacecraft orbital rate, the reported attitude will now include the error sources listed in 'l'able 3, in addition to NEA. This category of dynamically driven errors defines the relative accuracy of the ASC.

Table 3. ASC dynamic error sources

- Star catalog error
- Abberation correction error
- Lens chromatic error
- Lens geometric correctioin residual error
- CCD pixel to pixel variations
- Centroiding residual
- Close object fusing
- False object lock
- Time stamp uncertainty

Boresight Bias and Absolute Accuracy

Finally, long term effects, typically caused by thermal or mechanical stressing, will affect the boresight pointing knowledge or bias. The time scale of them effects can cover the span from manufacturing calibration to end of life, including launch induced effects. When these. c. ffects arc added to relative. accuracy, the. resulting summation of all errors is defined as the absolute accuracy. Since they arc largely long term effects, they may be regarded as being a bias, and are added linearly (rather than in an RSS manner) to the other error terms. It should be noted that calibration) uncertainty is a component of the total bias Set.

The ASC CHU uscs a unique, kinematic mounting system which has a positional accuracy, and stability, in the low aresecond range. It uses three, precision, ceramic balls. The boresight accuracy achieved by this system is at least one order of magnitude better than conventional, planar mounts. The usc of the ball kinematic mount is enabled by the very low power and mass of the CHU.

Lifetime and other Noise Effects

Aging and radiation decrease accuracy on both a short term and a long term basis. 1 lence, both the begin of life (BOL), and the. end of life (EOL) values must be recognized.

Since the ASC determines its attitude based on all of the. bright stars in its FOV, the accuracy of the instrument relies on both the accuracy of the determination of each individual star centroid, and on the accuracy of the centroid to star catalog matching.

Generally, the impact on the overall accuracy of the noise of a single star centroid will be reduced by the square root of the number of stars used, due to the. averaging in the ASC. 1 lowever, a few of the error sources are systematic and therefore, do not show this property, such as the boresight bias terms.

The effect of noise. on the precision of the matching algorithm has an even more complex effect. important factors arc 1 .SF residual, false objects and/or missing links between centroids and catalog entries, and, also, catalog errors themselves. These errors affect the accuracy in three different ways:

1) A bright star is always detected and linked reliably. Hence, a catalog error will affect the attitude dc.termination as long as the. star remains in the FOV. For the attitude determination, this will appear as a relative attitude error (reduced by the square root of the number of stars in the FOV).

2) A dim star at just above the detection limit, will be detected and linked in some images and not on others due to noise. This will result in an effective increase in NEA and is inelude.d in the NEA values quoted in Table 2, except for the ASC-I 11', as mentioned below. This will also apply to other noise sources such as proton induced charges (radiation) and other false objects such as satellites in the 1 'OV. However, it should be noted that some of these increases in NEA may be eliminated in future applications where a very low, staring N} 'A is critically important to the mission. An example of this is the. AS~-11 P, where the projected NEA assume.s implementation of staring mode operation.

3) A moving star field will have stars entering and leaving the FOV. For the ASC, the offset of one star changing at a time only results in a minor, N}iA-like, effect on pointing accuracy, because of the large number of stars being tracked. 1 'or a conventional star tracker this ef-

feet is pronounced and causes accuracy dominating jumps in the pointin g position [9]. The analog like response of the ASC to a changi ng number of stars being tracked effectively suppresses these jumps and provide.s a smooth attitude report with time and position changes.

7. Acquisition Performance

The performance of the lost in space (1 .1S) algorithm was measured for most of the data frames taken in Mauna Kea and TMO test series. The 1 .1S needs to deliver the attitude solution within 0.3" of the true pointing direction in order to assure a successful handoff to the CSF algorithm. Therefore, the performance of the 1.1S algorithm was judged by both a comparison to the estimated attitude angle value ant] the convergence of the CSF.

The two examples of 1 .IS algorithm performance were both taken with zenith pointing at Mauna Kca, over a period of hours, with the star field changing at the sidereal rate. 1 During that time, the star field motion covered 3 ASC FOVs.

Out of 2581 images which were analyzed, the 1 .IS algorithm only failed for four data frames. All four occurred while pointing at a very meager star field (1 ig. 5). The first two failures contained light tracks from airplanes in two of the failed frames and a transient, telescope dome light caused severe interference in the other two failed frames. The lost frames were a good test of the acquisition autonomy, reliability and robust-ness, since the acquisition valid flag dropped for these four frames, and only these four frames, from all of the. test series.

1 ig. 6 shows total acquisition success on a rich star field on a TMO run. The number of stars acquired by the 1.1S is 20 to 32.

It should be noted that the tracking data base includes five times the number of stars as the acquisition data base, so that the number from which the attitude quaternion is derived is much larger than the number required for acquisition.

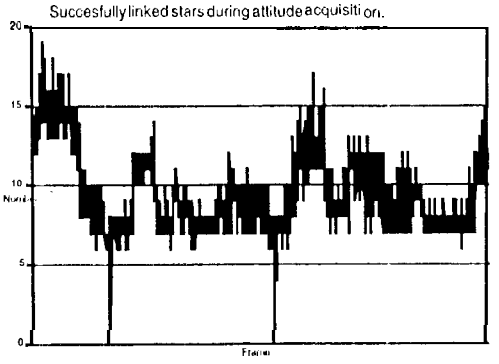

Figure 5. Number of stars recognized during acquisition in a meager star field, zenith pointing, Mauna Kea.

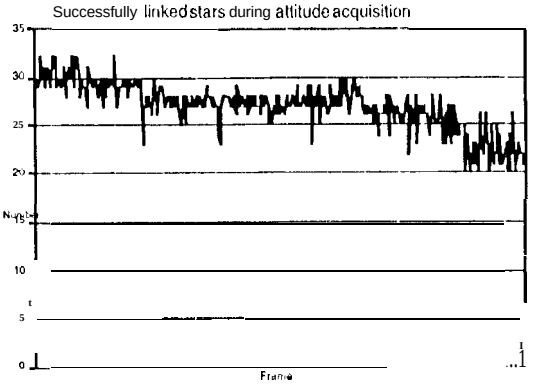

Figure 6. Number of stars recognized during acquisition in a rich star field, zenith pointing, TMO.

In summary, the reliability and robustness of the acquisition process have been demonstrated. In the four frames, out of the thousands, when acquisition did not occur, for various reasons, the failure was accurately reported by the appropriate. flag status. The acquisition success in space can be expected to be even higher, because of the elimination of ground based artifacts.

8. Measured Accuracy

The ASC has been evaluated at the JPL operated, 'J'able Mountain Observatory facility which is located at Wrightwood, California on several occasions [5]. 1 lowever, in June 1996, the ASC tested at the observatories of the University of Hawaii on Mauna Km, Hawaii [1 ()]. The purpose of the. test was to determine the accuracy of the ASC with a minimal perturbing airmass and the highest possible qual-

ity of "seeing" [11]. These desirable evaluation conditions are available on Mauna Kea.

Two kinds of accuracy were determined with the real sky tests: the NEA and the relative accuracy. The NEA was measured utilizing a telescope as an ASC mount and tracking a specific, fixed, part of the sky. The tracking data gathered at Mauna Kea included 727 images. As an example, the uncorrected declination output is shown in Fig. 7.

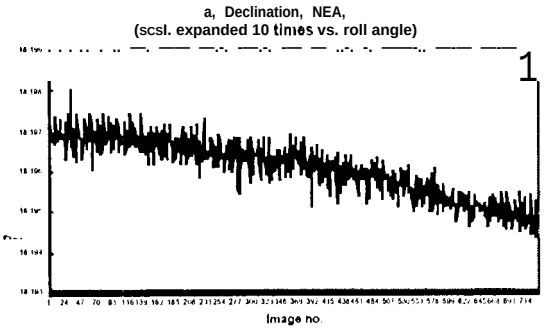

Figure 7. Uncorrected tracking series of declination measurements.

Relative accuracy was the other parameter which was evaluated. The noise in pointing knowledge. with a changing star field, which is the relative accuracy, was measured by pointing the star camera toward the zenith and acquiring continuous attitude data while stars drifted through the camera FOV at the sidereal rate. When the epoch of the star catalog is the same as the observing time, the declination and roll angles remain constant, whereas the right ascension increases with the side.rc:il rate. The data acquired at Mauna Kea included a zenith pointing series in excess of 2 hours and 2578 images. As an example, the. uncorrected declination angle is shown in 1 figure 8.

It should be noted that the data were acquired over a period of hours. This means that artifacts such as air stability, thermal displacement of the camera, changing moon light, and telescope drift are also included in the uncorrected attitude angles. These phenomena are not directly related to the instrument performance and must be subtracted from the raw data in order to determine the true instrument performance. Generally, these effects vary slowly with time and can be subtracted from the signal by utilizing Fourier transforms [1 0]. The effect of applying a 0.005 1 Iz filter to the zenith pointing data series is shown in Fig. 9. The remaining signal is a more accurate representation of the inherent performance of the instrument. It is difficult to define a specific frequency boundary between external artifacts and internal instrument errors, bc.cause the artifacts are not well quantified. However, a conservative performance estimate based on the statistics of the attitude output, is given in Table 4.

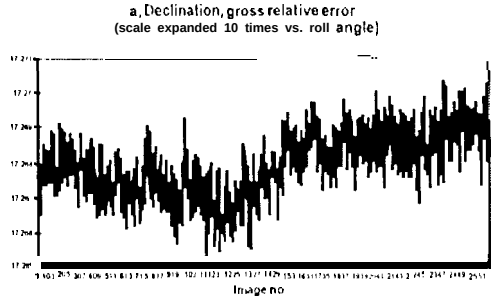

Figure 8. Uncorrected zenith series of declination measurements.

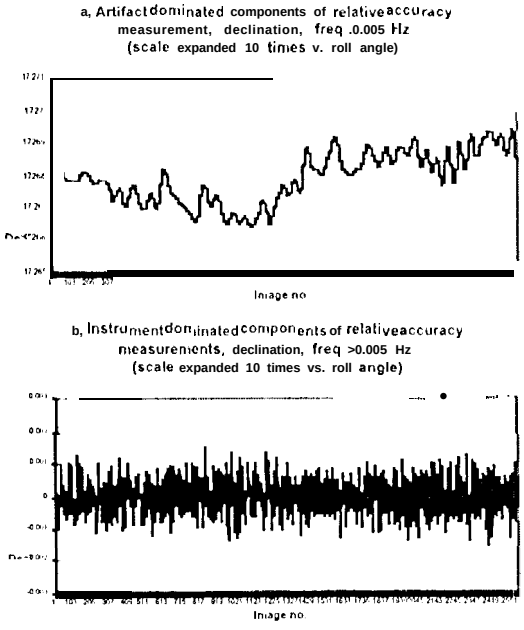

Figure 9. Slow and fast varying components of declination angles from the zenith pointing series. ASC relative accuracy is represented in b.

'1'able 4. ASCPerformance **Summary**

Parameter	NEA (arcsec, RMS)	Relative accuracy (arcsec RMS)
Declination	1.1	1.4
Right ascension	1.2	NA
Roll Angle	8	13

As the absolute instrument accuracy is in the range of a few arcseconds, it surpasses most mechanical attitude transfer systems. Therefore, for the telescope tests, only the NEA and the relative accuracy can be assessed. Because of telescope thermal mechanical pointing changes, which dominate those of the ASC and nullify any attempt to measure the ASC boresight bias terms, the boresight bias drift and offset accuracy terms cannot be measured in this manner.

9. CONCLUSIONS

The fully autonomous ASC differs from conventional star trackers because it solves the lost in space problem internally, because it outputs the attitude directly in celestial coordinates, because of its unusually fast optics, because it is a true multi-star tracker, and because it separates the detection and processing functions in separate units. It thus qualifies as the first example of a second generation, solid state, star tracker.

Two diffc.rent kinds of noise were evaluated at Mauna Kea Observatory, Hawaii. These were the NEA and the relative accuracy of the ASC.

The absolute pointing accuracy of the AS(is superior to larger star trackers with smaller FOVs, because the ASC utilizes a large number of stars in the FOV and because the small size, low power dissipation and very stable mount of the ASC CHU enable the realization of exceptionally good mechanical and thermal mechanical stability.

Robust initial acquisition was demonstrated on both meager and rich star fields at Mauna Kea.

While the ASC was developed to meet the nc.eels of the Ørsted mission, it can be beneficially used on a wide range of spacecraft .

10. ACKNOWLEDGMENTS

This work has been sponsored by 1 ESTEC (Contract no. 15 1713), the RadioParts Foundation, the Technical University of Denmark, anti NASA Code YSG. The research described in this publication was carried out in part by the Jet Propulsion 1 aboratory, California Institute of Technology, under a contract with the National Aeronautics and Space Administration.

1] . REFERENCES

[1] The Ørsted Satellite, Brochure, Computer Resources International, Birkerød, Denmark 1994.

[2] 0. V. Nielsen et al: Development, construction and analysis of the Ørsted fluxgate magnetometer, *Measurements Science Technology*, 6. (1 995), p. 1 099-1115.

[3] I, 1 aursen: The Overhauser Scalar Magnetometer, Proceedings 1st Ørsted International Science Team Meeting, Copenhagen, June 6 8, 1995.

[4] 1). Stauning: Charged Particle Detectors, Ørsted system design **Ic.view,** Birkerød, Denmark, October ?1 - 2?, 1992.

[5] A. R. Eisenman; C. C. Liebe; J. L. Jørgensen: Astronomical Performance of the Engineering Model Ørsted Advanced Stellar Compass, Proceedings of SPIE vol. 2810, 6 8 August 1996, Denver, Colorado, p. 252- 262.

[6] C. C. Liebe: Star '1'rackers for Attitude Determination, *IEEE A erospace and Electronics Magazine*, June 1995, p. 1016.

[7] C. C. 1 iebe: Pattern **Recognition** of Star Constellation for Spacecraft Applications, *IEEE Aerospace and Electronics Magazine*, January 93, p. 31-39.

[8] M. D. Shuster; S. D. Oh: Three-Axis Attitude Determination from vector Observations, *Journal of Guidance, Control, and Dynamics*, Volume 4, No. 1, p. 70 77.

[9] T. E. Strikwerda; H. L. Fisher: Analysis of the NEAR star tracker flight data; SPIE proceedings vol 2810, p. 265- 273, Denver, Colorado, 6 8 August 1996.

[10] A. R. Eisenman; C. C. Liebe: operation and Performance of a Second Generation, Solid State, Star Tracker, the. ASC, proceedings of international Symposium of the International Academy of Astronautics (IAA), Berlin, November 4 8, 1996.

[11] J. Kovalensky: Modern Astrometry, Springer Verlag, 1995.

12. BIOGRAPHIES

Allan Read Eisenman has been working in the field of electro-optics, at the Jet Propulsion Laboratory, since 1964, where he is a Group 1 matter and on the Technical Staff of the. Avionic Equipment Section. He has done pioneering development work on CCD star trackers in the early and mid 1970s and is currently engaged in the development of highly miniaturized and ultra precise, autonomous, CCD and Active Pixel Sensor based star and target trackers. Mr. Eisenman has both bachelor and master of science degrees from the UCLA school of engineering where he specialized in electronics.

John Leif Jørgensen is associate professor in image processing at the Technical University of Denmark (DTU). He received a masters degree in Engineering/Physics from DTU in 1981 and BBA from Copenhagen School of Commerce in 1987. He is the principal investigator on the ASC for the. Ørsted satellite and the Swedish ASTRID II satellite.

Carl Christian Liebe was born in Copenhaagen 1966. Currently he is an assistant professor of the Institute of Automation at the 'Technical University of Denmark. He received a masters degree in Electrical Engineering in 1991 and a Ph.D. in 1994, both from DTU. He is coinvestigator on the ASC for the Ørsted Satellite and the Swedish ASTRID II satellite..

Gunnar Bent Jensen is lecturer in Physics at the Technical University of Denmark. He was born in Jutland, Denmark in 1929. He received his masters degree in theoretical physics at the Niels Bohr Institute in 1955. His interests are quantum physics, diffraction theory and practice, and fast algorithms for computing.